IMPACT CONTROL DURING THE CONTACT TRANSITION OF A FLEXIBLE LINK MANIPULATOR

Carlos E. Ingar Valer
Pontifícia Universidade Católica do Rio de Janeiro, PUC-Rio,
Departamento de Engenharia Mecânica.
cingar@mec.puc-rio.br

Rubens Sampaio
Pontifícia Universidade Católica do Rio de Janeiro, PUC-Rio,
Departamento de Engenharia Mecânica.
rsampaio@mec.puc-rio.br

Abstract. *In this paper we propose a control strategy to deal with impacts in flexible robot manipulators during the transition from a free motion to a constrained motion. Impacts are undesired because they induce large interaction forces, which are harmful to robot manipulators and the environment. Moreover, the high energy of the robot manipulator when it impact the environment must be dissipated in a very short time and conventional force controllers are not prepared to deal with this problem. Here, in this paper, it is investigated the use of a structural control strategy to help to dissipate the maximum quantity of energy during the contact transient. This controller is tested in a flexible robot manipulator where it is considered the use of piezoceramic plates glued on the flexible link of the manipulator. These piezoceramic plates, which have the piezoelectricity as an inherent property, will play the role of both actuators and sensors for the structural vibrations in the flexible link. The controller structure was chosen in such way that spillover phenomenon is avoided, and it was designed through the use of a parameter optimization algorithm, which is formulated as a non-linear programming problem. Simulations performed in MatLab® show the effectiveness of the proposed strategy.*

Keywords*: impact, flexible manipulator, piezoelectricity, structural control, optimization.*

1. Introduction

There are two extreme operational modes for robotic manipulators: position controlled motion through the free space, and force controlled interaction while constrained by the environment. In the first mode the manipulator moves in free space without any interactions with the environment and it is useful to perform tasks such as welding, painting, etc. In this mode, the controller objective is to place the end-effector on a specified position. The second mode is used to perform tasks such as assemblies and finishing operations, and in this mode, the controller objective is to maintain a desired contact force while the manipulator end-effector makes contact with the environment. Obviously the manipulator must change from the unconstrained mode to the constrained mode readily and during the transition impact and lost of contact occurs (see Fig. 1-a). During the transient phenomena more that one impact could occurs, and each one of theses takes place in a very short period, and are characterized by high contact forces and energy transfer which are undesired because they could be harmful for the robot and environment.

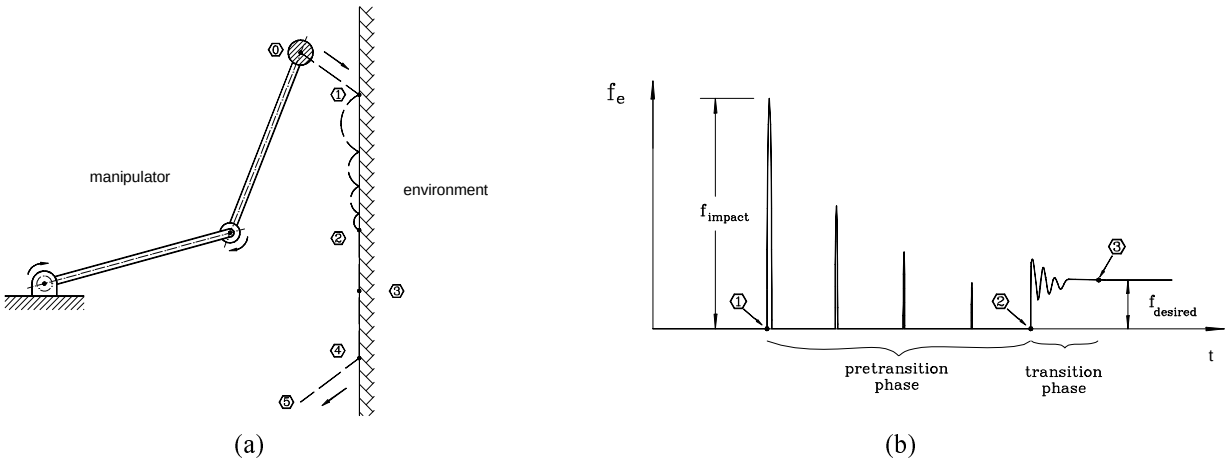

(a) (b)

Figure 1. Contact transition of a robot manipulator

In the past, the manipulators has been controlled to move slowly in order to avoid or reduce the impacts severity, but the increasing demand for high velocity of tasks execution makes the impacts unavoidable. Typically, it is the force controller which has to deal with the transition phenomena from the instant the first impact is detected, however the transferred energy must be dissipated in a very short time and conventional force controllers are not prepared to deal with this problem neither with the contact losses. The problem of development of control strategies for the contact transition in robotic manipulators has been widely ignored for many years. In the previous research, just a few attempts to improve the quality of the contact transient in robot manipulators have been done and it still represents a open problem. Matter gets more complicated when link or joint flexibility that which created undesired vibrational effects, is present.

Figure 1-b shows a typical diagram for the impact/contact force history during the contact transition of the robot manipulator shown in Fig. 1-a. As can be seen in Fig. 1-b, it can be distinguish two phases: pre-transition and transition phase. During the pre-transition phase, many contact losses can occur, and during the transition phase, they don't occur but the desired force level is not maintained yet because of the natural elasticity of the contact. Based on Fig. 1-b, the objectives of a transition controller can be established: To drive the manipulator against the environment surface avoiding large force peaks and contact losses (i.e. to improve the quality of the pre-transition phase), while increasing the contact force from zero to the desired force level as rapidly as possible.

Some previous works showed that the joint damping is beneficial and effective during the contact pre-transition because it can help to damp the high frequency oscillations of the manipulators, and then diminishing the number of contact losses (Oh, 1999)(Volpe and Khosla 1995). However, these researchers considered manipulators rigid enough and they did not consider the case of more flexible manipulators. A simple analysis with a simplified model for a flexible manipulator, as shown in Fig. 2, revels that the joint damping, represented by B_1 is not effective for transition control in flexible manipulators when the manipulator stiffness, represented by K_m is small when compared to the environment stiffness, represented by K_e.

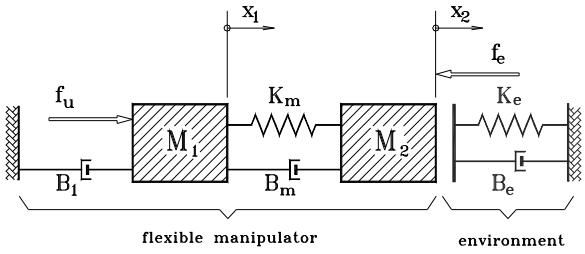

Figure 2. Simplified model for a flexible robotic manipulator interacting with its environment

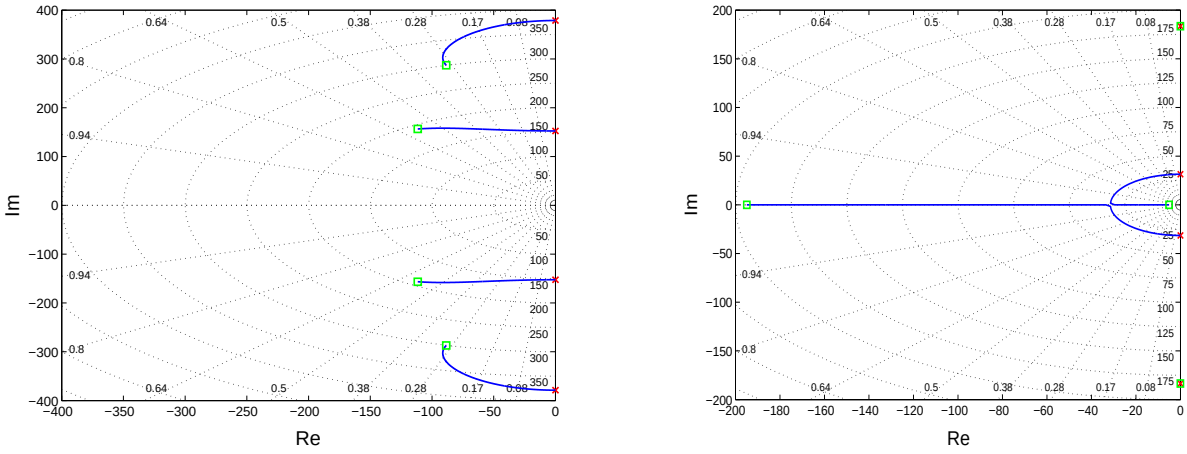

(a) (b)

Figure 3. Root locus for the simplified flexible manipulator model varying the joint damping B_1 only. (a) Not very flexible manipulator ($K_m / K_e = 1$). (b) Very flexible manipulator ($K_m / K_e = 0{,}01$).

As can be seen from Fig. 3-a, when the flexibility is small, i.e. $K_m / K_e = 1$, the joint damping is effective to damp both of the two flexible modes (and this way improving the contact transition quality). However, when the flexibility is considerable, i.e. $K_m / K_e = 0{,}01$, the joint damping cannot damp the highest frequency mode. In this work, we

proposed a structural control strategy to help to dissipate the maximum quantity of energy during the pre-transient contact phase of a flexible manipulator. This controller helps to improve the contact transient quality. To this, it is considered the use of piezoceramic plates glued on the flexible link of the manipulator that play the role of both actuators and sensors for the structural vibrations in the flexible link. The controller structure was chosen in such way that spillover phenomenon is avoided, and it is designed through the use of a parameter optimization algorithm, which is formulated as a non-linear programming problem.

2. The system model

The system to study is shown in Fig. 4-a. As can be seen, it consists of a flexible link manipulator that contacts its environment. Piezoelectric plates, glued along the flexible link, will be used as actuators and sensors. In those figures, L_b represents the link length modeled as a flexible beam, E_bI_b the beam stiffness, and m_b the beam mass per unit length, J_h, B_h and r_h the joint inertia, joint damping and radius respectively, M_t and $J_{t,G}$ the tip mass and rotational inertia in relation to its own mass center, respectively. θ represents the angular displacement and f_e the contact force (exerted by the manipulator over the environment). The dimensions of the piezoelectric plates are defined by the variables a_p, b_p and s_p and is location is defined by x_p as showed in Fig.4-a and Fig. 4-b.

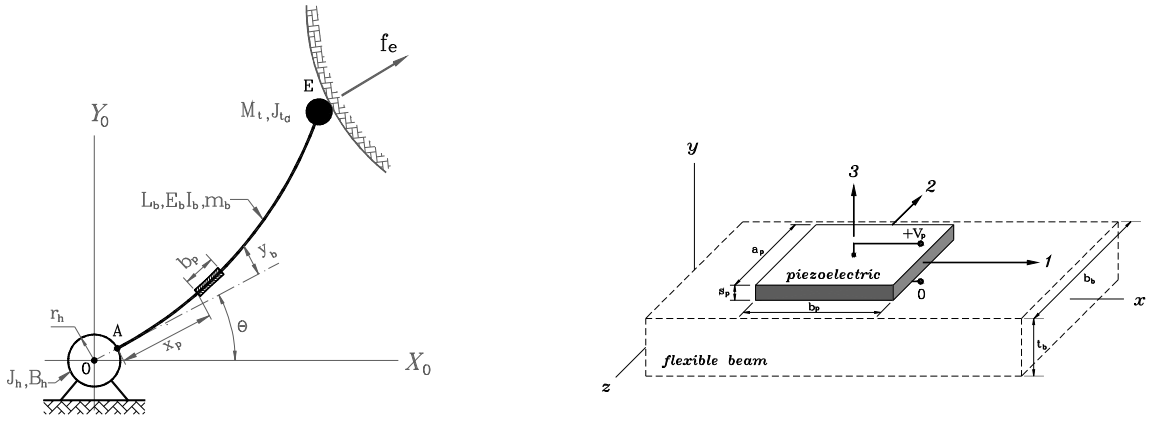

(a) (b)

Figure 4. Single-link flexible manipulator including glued piezoelectric plates and contact with its environment

2.1. Motion equations for the flexible manipulator including piezoelectric plates

The manipulator was modeled by using the Lagrange Equations (Kalaba, 1996). The flexible link is considered as an Euler-Bernoulli beam (Inman, 1996) and it was used the Assumed Mode Method (Meirovitch, 1990) to define the beam displacements according to the following equation:

$$y_b(x,t) = \boldsymbol{\psi}^t(x)\ \mathbf{q_b}(t) \tag{1}$$

where, $y_b(x,t)$ is the beam displacement (see Fig. 4-a), $\mathbf{q_b}(t) = [q_1(t), \cdots, q_N(t)]^t$ is the vector of modal coordinates with N the number of assumed flexible modes, and $\boldsymbol{\psi}(x) = [\psi_1(x), \cdots, \psi_N(x)]^t$ is a vector of appropriate comparison functions (Junkins, 1996). The detailed procedure to obtain the motion equations can be found in the work of Valer, 2004. Here we only present the results. They are given by the following set of coupled equations:

$$J_h\ddot{\theta} + \tilde{\boldsymbol{\psi}}^t\ddot{\mathbf{q}}_b + B_h\ \dot{\theta} + \mathbf{J}_\theta{}^t(\theta, \mathbf{q_b})\ \mathbf{f_e} = \tau \tag{2}$$

$$\mathbf{M_b}\ \ddot{\mathbf{q}}_b + \tilde{\boldsymbol{\psi}}\ \ddot{\theta} + \mathbf{K_b}\ \mathbf{q_b} + \mathbf{J}_{q_b}{}^t(\theta, \mathbf{q_b})\ \mathbf{f_e} = \overline{\mathbf{B}}_p\ \mathbf{v_{pa}} \tag{3}$$

where $\boldsymbol{\tau}$ is the control torque applied on the manipulator joints and $\mathbf{v_{pa}}$ the applied voltages on piezoelectric actuators. $\mathbf{M_b} = \mathbf{M_b}^t > \mathbf{0}$ and $\mathbf{K_b} = \mathbf{K_b}^t \geq \mathbf{0}$ are the combined beam/tipmass inertia and stiffness matrices when the link is considered clamped on point A, respectively. $\tilde{\boldsymbol{\psi}}$ is a coupling parameter which is function of the comparison

functions $\boldsymbol{\psi}$. $\mathbf{J}_\theta$ and $\mathbf{J}_{q_b}$ the Jacobian in relation to θ and $\mathbf{q_b}$, and $\overline{\mathbf{B}}_\mathbf{p}$ the piezoelectric distribution matrix which is function of piezoelectric physical properties and geometry. Expressing Eqs. (2) and (3) in a compact form, we have:

$$\mathbf{M(q)}\ \ddot{\mathbf{q}} + \mathbf{B}\ \dot{\mathbf{q}} + \mathbf{K}\ \mathbf{q} + \mathbf{J_e}^t(\mathbf{q})\ \mathbf{f_e} = \mathbf{B}_\tau\ \tau + \mathbf{B_p}\ \mathbf{v_{pa}} \tag{4}$$

with

$$\mathbf{q} = \begin{bmatrix} \theta \\ \mathbf{q_b} \end{bmatrix} \tag{5}$$

$$\mathbf{M(q)} = \begin{bmatrix} J_h & \tilde{\boldsymbol{\psi}}^t \\ \tilde{\boldsymbol{\psi}} & \mathbf{M_b} \end{bmatrix},\ \mathbf{B} = \begin{bmatrix} B_h & \mathbf{0} \\ \mathbf{0} & \mathbf{0} \end{bmatrix},\ \mathbf{K} = \begin{bmatrix} \mathbf{0} & \mathbf{0} \\ \mathbf{0} & \mathbf{K_b} \end{bmatrix},\ \mathbf{J_e}^t(\mathbf{q}) = \begin{bmatrix} \mathbf{J}_\theta^{\,t} \\ \mathbf{J}_{q_b}^{\,t} \end{bmatrix},\ \mathbf{B}_\tau = \begin{bmatrix} 1 \\ \mathbf{0} \end{bmatrix},\ \mathbf{B_p} = \begin{bmatrix} 0 \\ \overline{\mathbf{B}}_\mathbf{p} \end{bmatrix} \tag{6}$$

For collocated piezoelectric actuators/sensors, the piezoelectric voltages measured by the sensors, denoted by $\mathbf{v_{ps}}$, are given by (Valer, 2004),

$$\mathbf{v_{ps}} = \alpha\ \overline{\mathbf{B}}_\mathbf{p}^{\,t}\ \mathbf{q_b} \tag{7}$$

where α is a positive constant which depends of the relative size between the piezoelectric sensors and actuators.

2.2. Impact/contact model

To model contact forces, we choose the Hertz law which provides the following equation to compute the contact forces $\mathbf{f_e}$ as a function of deformation δ (see Fig. 5):

$$\mathbf{f_e} = \mathbf{K_e}\ \delta^{3/2} \tag{8}$$

(a) (b)

Figure 5. Deformation of contacting bodies. Hertz law.

Where, the constant $\mathbf{K_e}$ depends of physical properties and geometry of the contact bodies (Johnson, 1985).

3. Controller design

In this section is described the procedure to design the controller used during the contact transition of the robotic manipulator.

3.1. Control structure

The control structure is represented in Fig. 6. As it can be seen, it consists of two parts. The first one is an explicit proportional force controller with feedforward, which is useful to increase the contact force from zero to the desired level. It is given by the following equation:

$$\tau = \mathbf{J_e}^t\ \left[\ \mathbf{K_{pf}}\left(\mathbf{f_e}^d - \mathbf{f_e}\right) + \mathbf{f_e}^{\mathrm{d}}\ \right] \tag{9}$$

where, $\mathbf{K_{pf}}$ is the controller gain and $\mathbf{f_e}^{\mathrm{d}}$ is the desired contact force. The second part is an internal damping control for the flexible beam, through collocated piezoelectric actuators and sensors. This part of the controller has as objective to increase the beam damping and then the contact transition performance. This controller is given by the following equation:

$$\mathbf{v}_{pa} = -\mathbf{G}_1\ \mathbf{v}_{ps} - \mathbf{G}_2\ \dot{\mathbf{v}}_{ps} \tag{10}$$

with $\mathbf{G}_1$ and $\mathbf{G}_2$ as controller gains. By taking Eq.(3), ignoring rotating terms, we have:

$$\mathbf{M}_b\ \ddot{\mathbf{q}}_b + \mathbf{K}_b\ \mathbf{q}_b = \overline{\mathbf{B}}_p\ \mathbf{v}_{pa} \tag{11}$$

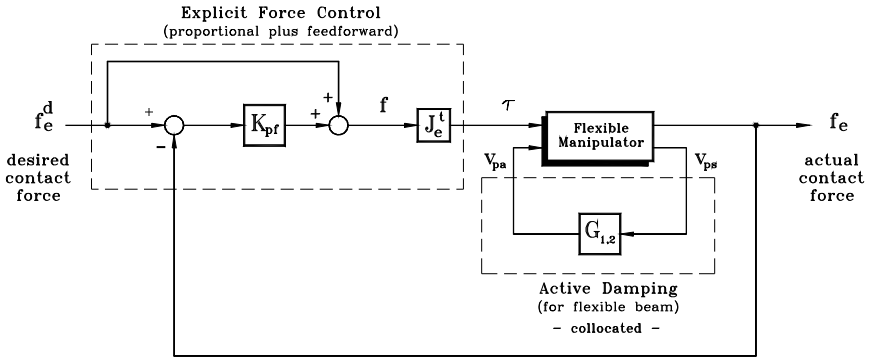

Figure 6. Block diagram for the proposed control system

Applying the active control law given by Eq.(10) in Eq.(11), we obtain:

$$\mathbf{M}_b\ \ddot{\mathbf{q}}_b + \left(\ \alpha\overline{\mathbf{B}}_p\ \mathbf{G}_2\ \overline{\mathbf{B}}_p^{\,t}\ \right)\dot{\mathbf{q}}_b + \left(\mathbf{K}_b + \ \alpha\overline{\mathbf{B}}_p\ \mathbf{G}_1\ \overline{\mathbf{B}}_p^{\,t}\ \right)\mathbf{q}_b = \mathbf{0} \tag{12}$$

By observing the last equation, we can concluded that if we choose the gain matrices as positive definite , i.e. $\mathbf{G}_1 = \mathbf{G}_1^{\,t} > \mathbf{0}$ and $\mathbf{G}_2 = \mathbf{G}_2^{\,t} > \mathbf{0}$, the collocated active damping control won't destabilize the system because the perturbation terms $\alpha\overline{\mathbf{B}}_p\ \mathbf{G}_2\ \overline{\mathbf{B}}_p^{\,t}$ and $\alpha\overline{\mathbf{B}}_p\ \mathbf{G}_1\ \overline{\mathbf{B}}_p^{\,t}$ are symmetric and positive definite matrices. This result is valid even if a reduced model is used for the flexible link, so the spillover phenomenon of flexible structures (Meirovitch, 1990) is avoided.

3.2. Optimization

From above, it is clear that a judicious selection of the gain matrices from the symmetric positive definite family guarantees the system stability. The most popular members of the family are the diagonal matrices, however, fully populated matrices allow commands to every actuator to be generated by linearly operating on all sensor measurements, and thereby provides significantly increased controller design freedom while stability is maintained and robustness in presence of residual dynamics is guaranteed. We can admit the most general positive definite gain matrices by introducing Cholesky descomposition:

$$\mathbf{G}_1 = \mathbf{R}\ \mathbf{R}^t \quad \text{and} \quad \mathbf{G}_2 = \mathbf{Q}\ \mathbf{Q}^t \tag{13}$$

with

$$\mathbf{R} = \begin{bmatrix} r_{11}^{\,2} & 0 & \cdots & 0 \\ r_{21} & r_{22}^{\,2} & \cdots & 0 \\ \vdots & \vdots & \ddots & 0 \\ r_{m1} & r_{m2} & \cdots & r_{mm}^{\,2} \end{bmatrix} \quad \text{and} \quad \mathbf{Q} = \begin{bmatrix} q_{11}^{\,2} & 0 & \cdots & 0 \\ q_{21} & q_{22}^{\,2} & \cdots & 0 \\ \vdots & \vdots & \ddots & 0 \\ q_{m1} & q_{m2} & \cdots & q_{mm}^{\,2} \end{bmatrix} \tag{14}$$

Let the following gain parameter vector:

$$\mathbf{p} = \left[\ r_{11}\ \ r_{21}\ \ \cdots\ \ r_{m1}\ \ r_{22}\ \ \cdots\ \ r_{mm}\ \ q_{11}\ \ q_{21}\ \ \cdots\ \ q_{m1}\ \ q_{22}\ \ \cdots\ \ q_{mm}\ \right]^t \tag{15}$$

Then, through Eqs.(13)-(15) it is clear that:

$$\mathbf{G}_1 = \mathbf{G}_1(\mathbf{p}) \quad \text{and} \quad \mathbf{G}_2 = \mathbf{G}_2(\mathbf{p}) \tag{16}$$

and the stiffness and damping matrices in Eq. (12) are also function of the parameter vector $\mathbf{p}$:

$$\hat{\mathbf{K}}(\mathbf{p}) = \mathbf{K}_b + \alpha \overline{\mathbf{B}}_p \; \mathbf{G}_1(\mathbf{p}) \; \overline{\mathbf{B}}_p^{\,t} \quad \text{and} \quad \hat{\mathbf{B}}(\mathbf{p}) = \alpha \overline{\mathbf{B}}_p \; \mathbf{G}_2(\mathbf{p}) \; \overline{\mathbf{B}}_p^{\,t} \tag{17}$$

then, Eq.(12) can be re-written as:

$$\mathbf{M}_b \; \ddot{\mathbf{q}}_b + \hat{\mathbf{B}}(\mathbf{p}) \; \dot{\mathbf{q}}_b + \hat{\mathbf{K}}(\mathbf{p}) \; \mathbf{q}_b = \mathbf{0} \tag{18}$$

The dynamic behavior of this system is determined by the following state matrix:

$$\hat{\mathbf{A}}(\mathbf{p}) = \begin{bmatrix} \mathbf{0} & \mathbf{I} \\ -\mathbf{M}_b^{-1}\hat{\mathbf{K}}(\mathbf{p}) & -\mathbf{M}_b^{-1}\hat{\mathbf{B}}(\mathbf{p}) \end{bmatrix} \tag{19}$$

It is known from linear systems theory that the performance of a system depends of the eigenvalues of its state matrix which, in our case, can be computed as function of the parameter vector $\mathbf{p}$. From the eigenvalue we can obtain the modal damped frequency and damping ratio which we denote here by $\omega_{di}(\mathbf{p})$ and $\varsigma_i(\mathbf{p})$, $i = 1 \ldots N$ respectively. A result of the control theory says that the robustness of a system to parameter perturbations depends on conditioning of the modal matrix of the closed loop state matrix $\hat{\mathbf{A}}(\mathbf{p})$ (Junkins, 1993). A measurement of the conditioning is the condition number defined by:

$$\kappa_{\hat{\mathbf{A}}}(\mathbf{p}) \equiv \frac{\sigma_M\left[\hat{\mathbf{\Phi}}(\mathbf{p})\right]}{\sigma_m\left[\hat{\mathbf{\Phi}}(\mathbf{p})\right]}$$

where $\hat{\mathbf{\Phi}}(\mathbf{p})$ denotes modal matrix and σ_M and σ_m maximum and minimum singular values, respectively. The condition number has the following property $1 \le \kappa_{\hat{\mathbf{A}}}(\mathbf{p}) < \infty$. Lower values of this number indicate better robustness. Based on these facts, we can formulate the problem of the determination of the parameter vector $\mathbf{p}$ as the following optimization problem:

$$\begin{aligned} &\textit{minimize} \;\; \kappa_{\hat{\mathbf{A}}}(\mathbf{p}) \qquad \textit{subject to} \\ &\mathbf{p} \in \mathrm{P} \qquad\qquad \omega_{di}(\mathbf{p}) \; \varsigma_i(\mathbf{p}) \;\ge\; \mu_i > 0, \qquad i = 1 \ldots m \\ &\qquad\qquad\quad \omega_{di}^{\,l} \le \omega_{di}(\mathbf{p}) \le \; \omega_{di}^{\,r}, \qquad i = 1 \ldots m \end{aligned}$$

with μ_i positive constants which are related to system response velocity or internal damping, $\omega_{di}^{\,l}$ and $\omega_{di}^{\,r}$ positive constants which represent left and right limits for the closed loop damped frequency. The optimization problem can be solved by using nonlinear programming solvers such as the Sequential Quadratic Programming algorithm (Bueskens and Maurer, 2000).

4. Numerical simulation results and analysis

In order to prove the efectiveness of the control strategy proposed in this work, a controller was designed by the procedure described above, and also a numerical simulation of the overall control system was performed. Tables 1 and 2 show the numerical values of the flexible manipulator and piezoelectric sheets parameters, and Fig. 8 shows the piezoelectric sheets distribution along the flexible arm.

The first two columns of Tab. 3 show the open loop natural frequency and damping ratio of the flexible manipulator arm. Because of the poor damping ratio, the goal of feedback controller was to increase the damping ratio to the target values shown on the third column of Tab. 3. After solving the optimization problem described in the previous section, the resulting natural frequencies and damping ratios were computed. This values are shown in the last two columns on Tab. 3.

Table 1. Main parameters used for the numerical simulation of the flexible manipulator

L_b [m]	t_b [m]	b_b [m]	$E_b I_b$ [N.m^2]	m_b [kg]	M_t [kg]	K_e (Hertz)
0,500	0,003	0,030	4,70	0,25	0,50	1x10^6

Table 2. Piezoelectric sheets parameters

Actuators				sensors			
a_{pa} [m]	b_{pa} [m]	s_{pa} [m]	material	a_{ps} [m]	b_{ps} [m]	s_{ps} [m]	material
0,030	0,100	0,001	PZT 5A	0,010	0,010	0,0005	PZT 5A

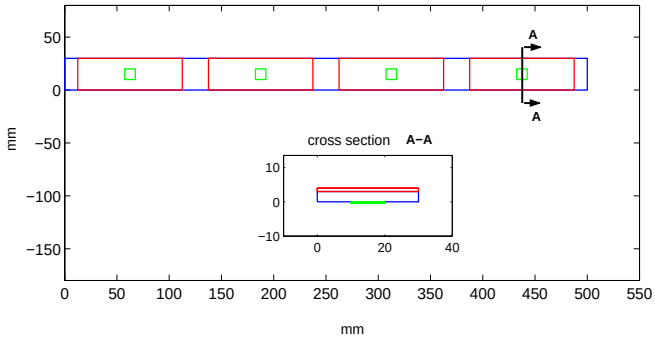

Figure 8. Piezoelectric sheets distribution along the flexible beam.
Blue: flexible beam, r*ed*: actuators, *green*: sensors.

Table 3. Characteristics of the flexible link

Open loop		desired*	closed loop	
ω_d^{open}	ς^{open}	$\varsigma^{desired}$	ω_d^{closed}	ς^{closed}
22,6	0,01	0,30	23,5	0,31
332	0,01	0,10	330	0,15
1021	0,01	0,10	1030	0,18
2030	0,01	0,10	2030	0,11

$* \omega_d^{open} - \Delta\omega \le \omega^{desired} \le \omega_d^{open} + \Delta\omega$, where $\Delta\omega = 5\%\ \omega_d^{open}$

As it can be seen, the closed loop values of natural frequency and damping ratio sucessfully overcame their target values. The simulation results of the flexible manipulator with the optimal controller implemented and subject to impact is show in the Fig. 9 and 10. In Fig. 9 it can be seen the endeffector displacements in both cases, without and with the optimal structural controller implemented. From this, it is evident that in the second case there are less impact, then less damage during the contact transition. This fact is confirmed in the Fig. 10-a, where it is showed that both, the number and intesity of impact forces decreased considerably.

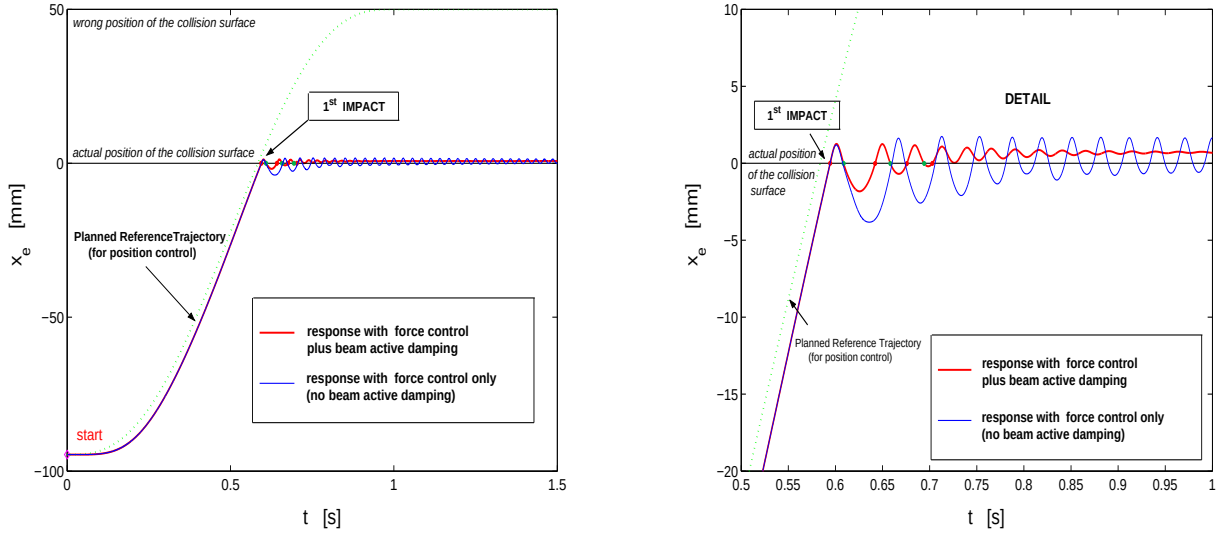

Figure 9. Manipulator end-effector horizontal displacement before and after an impact at 0,6 s.

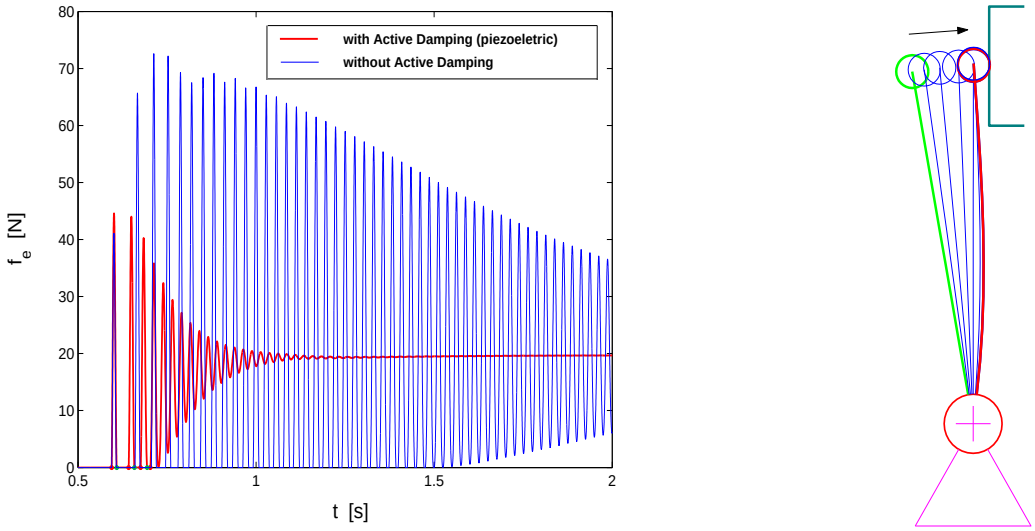

(a) (b)

Figure 10. (a) Impact/contact forces experienced by the flexible manipulator. (b) Flexible manipulator configurations during the transition

5. Conclusions

In this work, first it was argued that during the contact transition phase of robotic manipulators, the damping ratio is a critical factor that contributes to severity of impacts. Lower value of damping ratio, higher damage between the impacting bodies. However, it was showed that in the case of flexible robotic manipulators, it is hard to damp the flexible modes of vibration through the robot joint. Then, in order to overcome the damping ratio problem it was proposed a optimal control strategy which for the best of the authors knowledge was never tested before in impacting flexible manipulators. The results shown in this work proved the effectiveness of the strategy because it was observed that the number and severity of impacts can be decreased.

6. References

Bueskens, C. and Maurer, H., 2002, "SQP-Methods for Solving Optimal Control Problems with Control and State Constraints: Adjoint variables, Sensitivity Analysis and Real-Time Control", Journal of Computational and Applied Mathematics, Vol.120, pp. 85-108

Inman, D. J., 1996, "Engineering Vibration", Ed. Prentice Hall International Inc., 560 p.

Junkins, J. L. and Kim, Y., 1993, "Introduction To Dynamics and Control of Flexible Structures", American Institute of Aeronautics and Astronautics Inc., 452 p.

Meirovitch, L., 1990, "Dynamics and Control of Structures", Ed. John Wiley and Sons Inc., New York, 425p.

Ogata, K., 1993, "Engenharia de Controle Moderno", Ed. Prentice Hall do Brasil Ltda, Rio de Janeiro, Brazil, 781 p.

Oh, Y. H., Chung, W. K, "Analysis of a Robot System with a Passive Damper for Force and Impact Control". Advanced Robotics. 13(1): 1-23, 199.

Valer, C. I., 1997, "Controle Robusto H-inf de Estructuras Flexibles con Dinâmica Reduzida", XV COBEM, Aguas de Lindóia, SP, Brazil.

Valer, C. I., 2004, "Controle de Impacto em Manipuladores Robóticos", Ph.D. Thesis, Pontifícia Universidade Católica do Rio de Janeiro, Department of Mechanical Engineering, Rio de Janeiro, Brazil.

Valer, C. I., 2005, "Impact Force Identification in Flexible Strcutures by Using P-I Observer and Optimal Control", XI DINAME, Ouro Preto, MG, Brazil.

Volpe, R., Khosla, P., 2005. "The Equivalence of Second Order Impedance Control and Proportional Gain Explicit Force Control", The International Journal of Robotics Research, 14(6): 574-589, 1995.

7. Responsibility notice

The authors are the only responsible for the printed material included in this paper.